



This is a repository copy of *Ramification of thermal expansion mismatch and phase transformation in TiC-particulate/SiC-matrix ceramic composite*.

White Rose Research Online URL for this paper:
<https://eprints.whiterose.ac.uk/167452/>

Version: Accepted Version

Article:

Magnus, C., Sharp, J. orcid.org/0000-0001-8168-8422, Ma, L. et al. (1 more author) (2020) Ramification of thermal expansion mismatch and phase transformation in TiC-particulate/SiC-matrix ceramic composite. *Ceramics International*, 46 (12). pp. 20488-20495. ISSN 0272-8842

<https://doi.org/10.1016/j.ceramint.2020.05.151>

Article available under the terms of the CC-BY-NC-ND licence
(<https://creativecommons.org/licenses/by-nc-nd/4.0/>).

Reuse

This article is distributed under the terms of the Creative Commons Attribution-NonCommercial-NoDerivs (CC BY-NC-ND) licence. This licence only allows you to download this work and share it with others as long as you credit the authors, but you can't change the article in any way or use it commercially. More information and the full terms of the licence here: <https://creativecommons.org/licenses/>

Takedown

If you consider content in White Rose Research Online to be in breach of UK law, please notify us by emailing eprints@whiterose.ac.uk including the URL of the record and the reason for the withdrawal request.



eprints@whiterose.ac.uk
<https://eprints.whiterose.ac.uk/>

Manuscript Number: CERI-D-20-04548R1

Title: Ramification of thermal expansion mismatch and phase transformation in TiC-particulate/SiC-matrix ceramic composite

Article Type: Full length article

Keywords: Residual stress; Stress relaxation; thermal expansion mismatch; Phase transformation; ceramic composite; kink band

Corresponding Author: Dr. Carl Magnus,

Corresponding Author's Institution:

First Author: Carl Magnus

Order of Authors: Carl Magnus; Joanne Sharp; Le Ma; Mark Rainforth

Abstract: This article presents a microstructural study on the role of incipient residual stress relaxation in TiC-particulate/SiC-matrix ceramic composite toughened by thermal expansion mismatch and phase transformation toughening. Exhaustive microstructural studies was undertaken using scanning electron microscopy and transmission electron microscopy following a wear test. It was found that the superposition of hydrostatic tensile stress induced at the surface following the sliding contact on the inherent residual stresses locked in the composite led to a relaxation and/or reduction in the residual stresses. Stress relaxation presented a wider implication for the tribological properties of this ceramic matrix composite (CMC) in the form of a grain-scale rippling microstructural phenomena.

Dear Editor,

Many thanks for the opportunity to address the reviewers comments and recommendations. All latest corrections that have been carried out in the manuscript are highlighted in red text below the reviewers comment.

Reviewers' comments:

1. In the article title, SiC-TiC ceramic matrix could be added to clarify the research object of this article.

This has now been included in the title as advised

2. It was suggested some references that research on SiC based ceramic matrix could be added, like Ceramics International 46 (2020) 5159–5167 and so on.

This reference has now been included as advised

3. Please confirm if there is any sintering additive during the SPS process.

No sintering additives was employed and this has now been stated in the manuscript

4. Please add the heating rate of SPS process.

Heating rate 100 °C/min was employed and has been stated in the manuscript

5. It was suggested that a XRD result can be added in the article to investigate the phase transformation in larger scale than TEM.

XRD result has now been added to highlight phase transformation

6. It was suggested that the thermal expansion data of SiC and TiC could be added in the article.

A table showing thermal expansion data of all the phases in the composite system has now been added to the manuscript

Ramification of thermal expansion mismatch and phase transformation in **TiC-particulate/SiC-matrix ceramic composite**

Carl Magnus^{1,2*}, Joanne Sharp¹, Le Ma¹, W.M. Rainforth¹

¹The Henry Royce Institute and Department of Engineering Materials, The University of Sheffield,
Sir Robert Hadfield Building, Sheffield, S1 3JD, UK

²Anton Paar TriTec SA, Les Vernets 6, 2035 Corcelles-Cormondreche, Switzerland

Abstract

This article presents a microstructural study on the role of incipient residual stress relaxation in TiC-particulate/SiC-matrix ceramic composite toughened by thermal expansion mismatch and phase transformation toughening. Exhaustive microstructural studies was undertaken using scanning electron microscopy and transmission electron microscopy following a wear test. It was found that the superposition of hydrostatic tensile stress induced at the surface following the sliding contact on the inherent residual stresses locked in the composite led to a relaxation and/or reduction in the residual stresses. Stress relaxation presented a wider implication for the tribological properties of this ceramic matrix composite (CMC) in the form of a grain-scale rippling microstructural phenomena.

Keywords: Residual stress; Stress relaxation; thermal expansion mismatch; Phase transformation; ceramic composite; kink band

1. Introduction

Ceramic particulate composites have been extensively investigated for a number of years [1, 2]. However, a resurgence of interest and activity has arisen in the development of ceramic composite due to increased understanding of the limitations of some past composite approaches as well as the promising mechanical reliability such composite present as a result of the enhanced fracture toughness [3]. SiC-TiC: Silicon carbide titanium carbide compositions are seen as promising ceramic matrix composite system (CMCs) for re-entry applications, for example thrust chamber in rocket engines and thermal protection systems in spacecraft [4-6]. It has been hypothesized that: (1) the difference in properties, primarily thermal expansion, between SiC and TiC could lead to toughening by a microcracking thus improving thermal shock; and (2) the high hardness of the silicon carbide would impart erosion resistance. Subsequently, it has been realized that such a composite system might also

1 possess useful tribological applications, e.g. for seals, because of the reasonably low friction
2 coefficient of titanium carbide combined with good wear resistance of silicon carbide aided
3 by the reasonable lubricious rutile tribofilms [7].
4

5
6 The mechanisms that brings about toughening in particulate ceramic composites also carry
7 with them other ramifications which are often neglected in the development and application
8 of such composites [1]. It is well known that the mechanical properties of ceramics are a
9 complex function of the microstructure [2]. A microstructural feature that is often neglected
10 is internal residual stress [2]. Residual stresses are those that exist in the absence of applied
11 external forces and often occurs in all polycrystalline ceramics that have non-cubic structures,
12 have undergone a polymorphic phase transition, or include a second phase of different
13 thermal expansion [2, 8]. Microstresses play a vital role in ceramic matrix particulate
14 composites where mismatch in thermal expansion between the matrix and reinforcement may
15 be substantial [2]. Such internal stresses, which consists of both compressive and radial
16 components could be deleterious due to variation of the local microstructure at the grain size
17 level [8]. Although the compressive component is often beneficial as it acts to close a
18 propagating crack, whilst the tensile component if added directly to an applied stress could
19 assist in failure [2]. The magnitude of thermal expansion mismatch stress can be estimated
20 thus [9]:
21
22
23
24
25
26
27
28
29
30
31
32

$$\sigma_m = [(\alpha_m - \alpha_p)E_p V_p \Delta T] / \{1 + V_p(E_p/E_m - 1)\}$$

33
34
35
36 Where σ_m is the stress in the matrix, α_m and α_p are the thermal expansion coefficients of the
37 matrix and particle respectively, E_p and E_m are the elastic modulus of the particle and matrix,
38 V_p is the volume fraction of the particles and ΔT is the cooling range (i.e., difference between
39 the minimum temperature for plastic deformation and final temperature after cooling).
40
41
42
43

44
45 Stresses developed as a result of particle-matrix thermal mismatch and/or phase
46 transformation can significantly influence the degree of crack-particle interaction [1, 10].
47 This is because cracks tends to preferentially propagate normal to tensile stresses and parallel
48 to compressive stresses [3]. In other words, cracks are deflected around particles in
49 hydrostatic tension but attracted directly into particles subjected to hydrostatic compression
50 [3, 11]. As shown in Fig. 1, in (A); the crack is deflected around the particle under
51 hydrostatic tension. Whilst in (B); a propagating crack is attracted directly into the particle
52 under hydrostatic compression.
53
54
55
56
57
58
59
60
61
62
63
64
65

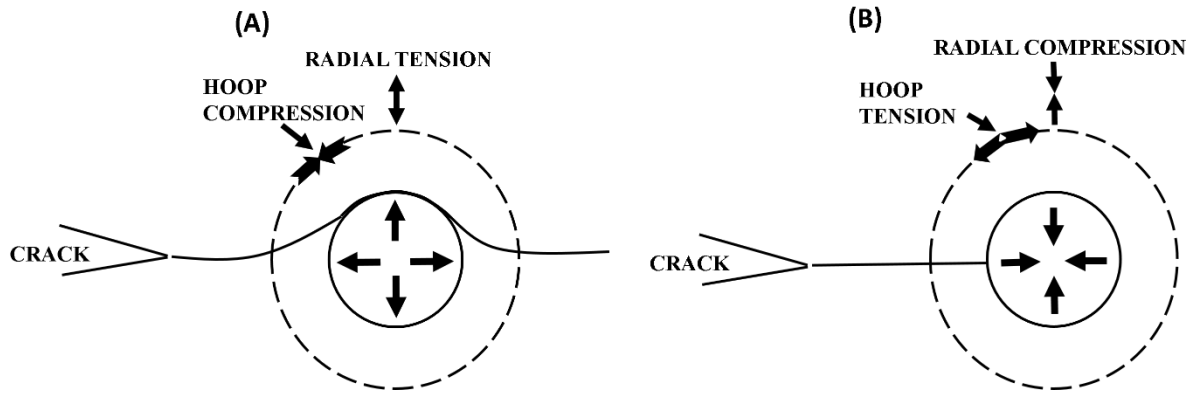


Fig. 1. Schematic of crack-particle interaction. (A) particle under hydrostatic tension ($\alpha_p > \alpha_m$) and (B) particle under hydrostatic compression ($\alpha_p < \alpha_m$). If the propagating crack does not fully relieve the compressive stress in the particle as shown in (B), then the interaction will effectively inhibit the motion of the crack, thus making this a much effective toughening mechanism due to crack impediment as compared to crack deflection in (a) [3].

Although residual stresses play an important role in fracture mechanism, however, they pose implications in many applications such as those involving localized phenomena [8]. As an example, in sliding wear applications, the combined shear and tensile stresses generated at a rubbing interface is significant with severe ramifications for the microstructure required [2, 8]. According to Lee et al.[2], residual stresses trapped in ceramic composites have a strong effect on wear as these stresses are added to the external applied stress. Compressive surface stresses which regenerate following further stress application enhances wear resistance [12]. However, as residual stresses initiated by thermal expansion mismatch are often locally tensile in nature [2], the subsequent addition of a strong tensile stress at the surface due to a sliding contact can lead to surface up-lift and microcracking – thus bringing about a catastrophic wear [2, 13].

Ultra-high structural materials often require ceramic composites to improve high temperature oxidation resistance. Understanding the role of residual stresses from thermal expansion mismatch between material phases is very crucial for maximizing structural integrity during service. Various aspects related to the improvement in mechanical properties most especially fracture toughness of ceramic matrix composites [14-21] have been well studied over the past years; however, few investigations have focussed on the potential stress relaxation of residual stresses due to the application of an external compressive and/or tensile stress. This work investigates the role of hydrostatic pressure during dry-sliding contact and its consequent

1
2
3
4
5
6
7
8
9
10
11
12
13
14
15
16
17
18
19
20
21
22
23
24
25
26
27
28
29
30
31
32
33
34
35
36
37
38
39
40
41
42
43
44
45
46
47
48
49
50
51
52
53
54
55
56
57
58
59
60
61
62
63
64
65

microstructural scale effect in SiC-matrix/TiC-particulate ceramic composite following spark plasma sintering (SPS) above the cubic to hexagonal SiC phase transformation temperature.

2. Experimental Procedure

2.1. Sample preparation and characterization

Consolidated SiC-50mol.%TiC matrix-particulate ceramic composite was produced through a powder metallurgy/SPS process, details elsewhere [22], but summarized as follow. Cubic SiC powder with mean particle size 1 μm and TiC powder mean particle size 2 μm were obtained from a standard commercial supply. The TiC and SiC powders were further milled together and sieved using a 200 mesh sieve to obtain a finer particle size. **The mixed powder was cold compacted in a 20 mm graphite die and consolidated using SPS at a heating rate of 100 $^{\circ}\text{C}/\text{min}$ from room temperature to a requisite sintering temperature of 2100 $^{\circ}\text{C}$ without sintering aids. The uniaxial load (54 MPa) was applied at room temperature and removed at the end of the dwell time (15 min).** Spark plasma sintering (SPS) has been utilized since it is readily available, typically produces refined microstructure and circumvents the use of sintering aids. **The relevant thermomechanical data of the starting material, namely TiC and β -SiC and the evolved phase α -SiC are presented in Table 1 [23].**

Non-lubricating wear test was conducted on the polished surface at ambient conditions using in ball-on-disc configuration. Details of the test conditions and parameters are discussed elsewhere [22]. Microstructural investigation of the as-synthesized and worn surface was carried out using scanning electron microscopy (SEM; Inspect F50, FEI The Netherlands) and transmission electron microscopy (JEOL JEM-F200 / 200 kV). The electron transparent TEM specimen from the pristine and worn surface was prepared using focused ion beam (FIB; FEI Helios NanoLab G3 UC, FEI company, The Netherlands). Further analyses which may be of interest can be found elsewhere [22] as the scope of this work is not a tribological study but instead the role of residual stresses on wear behaviour from a microstructural point of view.

Table 1. A summary of the key properties of TiC and SiC

Carbide	Crystal Structure	Young's Modulus (GPa)	Thermal Conductivity (Wm^{-1}K)	Thermal Expansion ($\times 10^{-6}/^{\circ}\text{C}$)	Vickers Hardness (GPa)	Melting Point ($^{\circ}\text{C}$)
TiC	Cubic	410 – 510	21	7.4	28 – 35	3067
β -SiC	Cubic	290 – 410	25.5	3.8	24.5 – 28.2	2545
α -SiC	Hexagonal	470	43	5.1	24.5 – 28.2	2545

3. Results

3.1. Phase Identification

XRD phase identification of the SPSed composite is shown in Fig. 2. As shown in the presented XRD pattern, the peaks of β – SiC and TiC are indistinguishable as they both crystallize in cubic structure. No evidence of solid solution between SiC and TiC was observed. However, the evolution of α – SiC peaks suggests cubic to hexagonal SiC phase transformation.

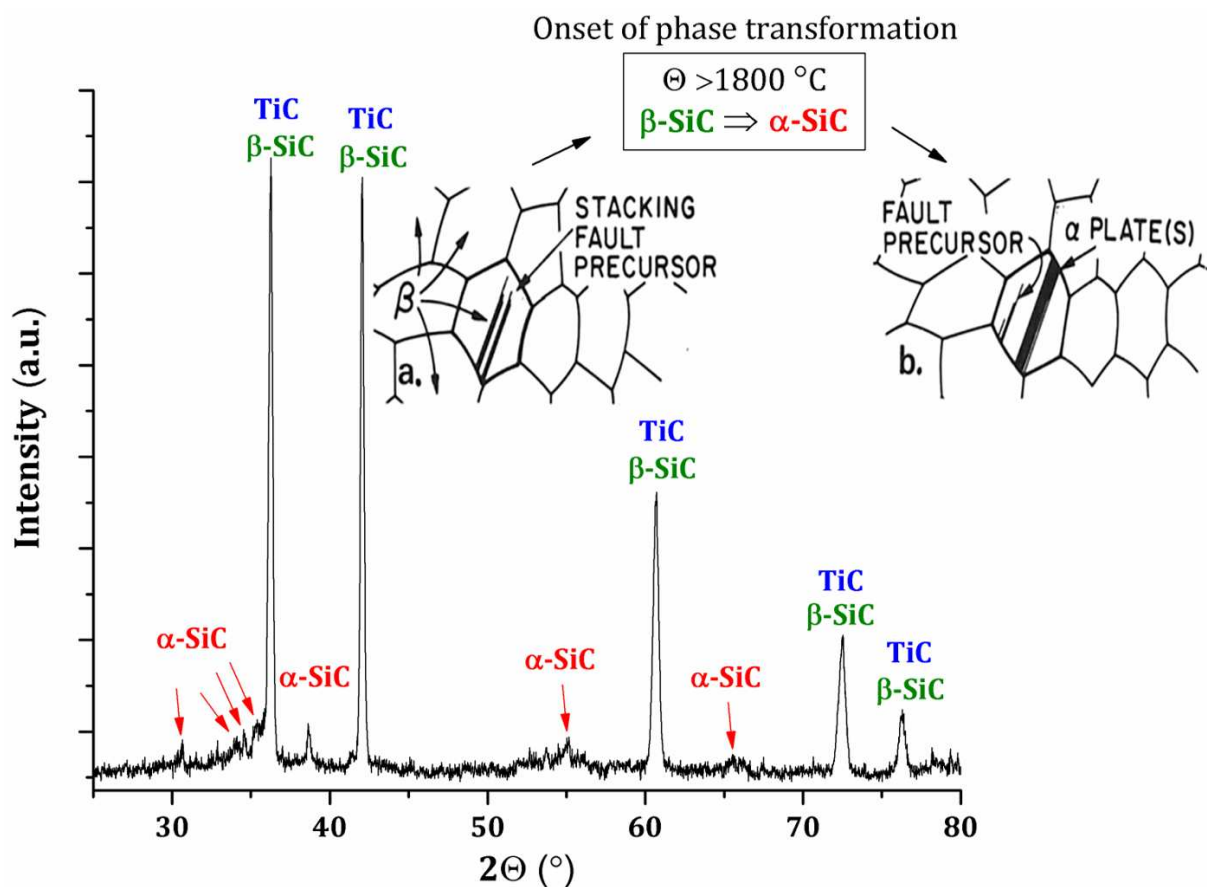


Fig. 2. XRD plot of the sintered compact. Inset shows schematically stages in the development of microstructure: (a) shows the formation of stacking fault in β – SiC – a precursor planar defect leading to the evolution of α – SiC, and (b) growth and formation of α – SiC plates.

3.1.1. As-synthesized microstructure

The microstructure of the as-synthesized unetched sample is shown in the secondary and corresponding backscattered electron micrographs in Fig. 3. According to EDS elemental map analysis presented elsewhere [22] the grey phase was the TiC grains whilst the dark phase was the SiC grains. The composite was nearly fully dense (99 %) with some pores

1
2
3
4
5
6
7
8
9
10
11
12
13
14
15
16
17
18
19
20
21
22
23
24
25
26
27
28
29
30
31
32
33
34
35
36
37
38
39
40
41
42
43
44
45
46
47
48
49
50
51
52
53
54
55
56
57
58
59
60
61
62
63
64
65

mainly along the grain boundary. The SiC grains appears to be elongated due to possible $\beta \rightarrow \alpha$ transformation as the sintering temperature exceeds 1800 °C as reported elsewhere [19]. The absence of any significant microcrack in the composite system implies that residual stress relaxation due to thermal mismatch between TiC and SiC as well as $\beta \rightarrow \alpha$ SiC phase transformation has not fully taken place.

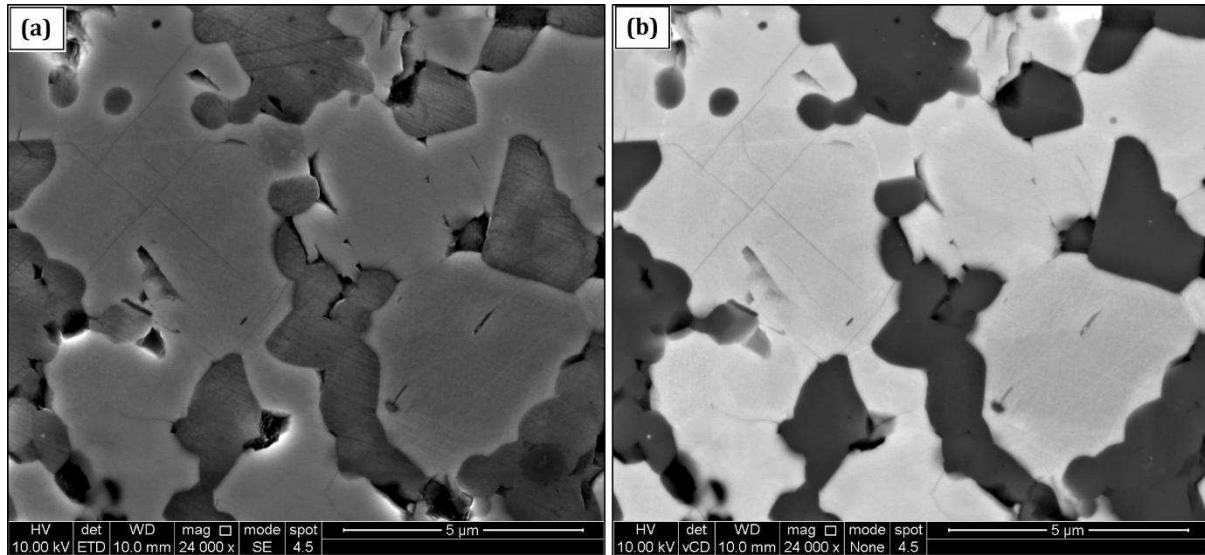


Fig. 3. Secondary electron (SE) and corresponding backscattered electron (BSE) micrographs obtained from the as-synthesized SiC-50mol.%TiC composite.

Site-specific FIB lift-out of the SiC grains from the pristine surface subsequently characterized by transmission electron microscopy for evidence of $\beta \xrightarrow{>1800\text{ }^\circ\text{C}} \alpha$ phase transformation is presented in Fig. 4. As shown in Fig. 4(a) and higher magnification Fig. 4(b) evidence of planar defects (i.e. stacking faults) can be seen in the SiC grains with corresponding electron diffraction pattern shown in the inset. Lattice fringe image (Fig. 4(c)) revealed partial SiC phase transformation as the growth of α – SiC took place epitaxially on the β – SiC particles. According to Heuer et al.[24], the stages in the development of microstructure during β – SiC to α – SiC phase transformation incorporates the glide motion of partial dislocation. The glide motion of partial dislocations across perfect β crystals will give rise to twins and stacking faults as observed in the HRTEM image (Fig. 4(d)) in consistent with observations reported elsewhere [24]. $[11\bar{2}0]$ zone axis electron diffraction pattern from the SiC grains (inset in Fig. 4(c)) revealed streaking and extra spots in the diffraction pattern linked to the evolution of the α polytype.

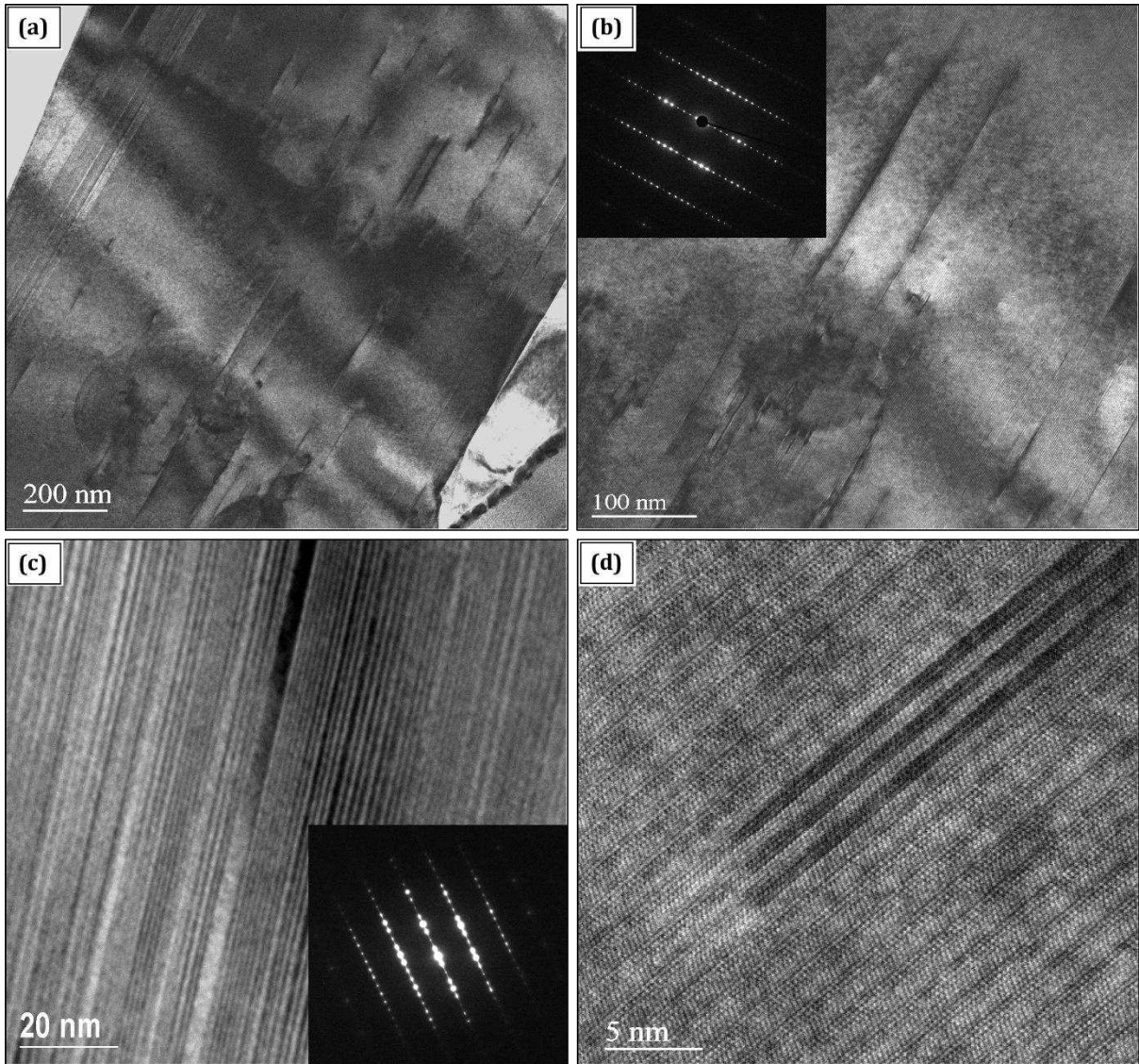


Fig. 4. (a) Bright field TEM image obtained from SiC grains; (b) higher magnification of (a) highlights stacking faults with inset showing the diffraction pattern of the β – SiC; (c) lattice image of the (0001) fringes showing partial $\beta \rightarrow \alpha$ phase transformation alongside α stacking sequences and faults and (d) HRTEM image of the interface between α and β SiC revealing stacking faults and twins.

3.2. Worn surface observations

3.2.1. Scanning electron microscopy and surface reconstruction

After performing a dry-sliding wear test, post-mortem worn surface characterization was undertaken using scanning electron microscopy as presented in Fig. 5. Secondary electron and corresponding backscattered electron micrographs (Fig. 5(a – c)) revealed stark evidence of preferential rippling of the TiC grains (white arrow) following the wear test. It appears that additional tensile stresses superimposed on the residual stresses locked in the composite system during the wear test led to the relaxation of the inherent tensile stresses around the

1 TiC grains - thus leading to surface up-lift manifesting as ripple formation as hypothesized
2 elsewhere [2]. As the thermal expansion coefficient of TiC is higher than that of SiC, during
3 cooling from the requisite sintering temperature TiC will cool faster than SiC. As a result, the
4 TiC grain will shrink faster than the SiC grain - thereby inducing tensile stresses in the TiC
5 grains and compressive stresses in the SiC grains. These residual stresses are locked in the
6 composite system and plays a vital role in improving the fracture toughness of this composite
7 system as reported elsewhere [11, 15]. The exact micromechanism(s) leading to ripple and/or
8 wrinkling of the TiC grains is not fully understood. However, it is plausible that the wear of
9 the compressive stress component (i.e. SiC grains (Fig. 6)) following the wear test alongside
10 the superposition of tensile stress originating from the sliding contact on the inherent tensile
11 stress locked in the TiC grains played a dominant role.
12
13
14
15
16
17
18
19
20
21
22
23
24
25
26
27
28
29
30
31
32
33
34
35
36
37
38
39
40
41
42
43
44
45
46
47
48
49
50
51
52
53
54
55
56
57
58
59
60
61
62
63
64
65

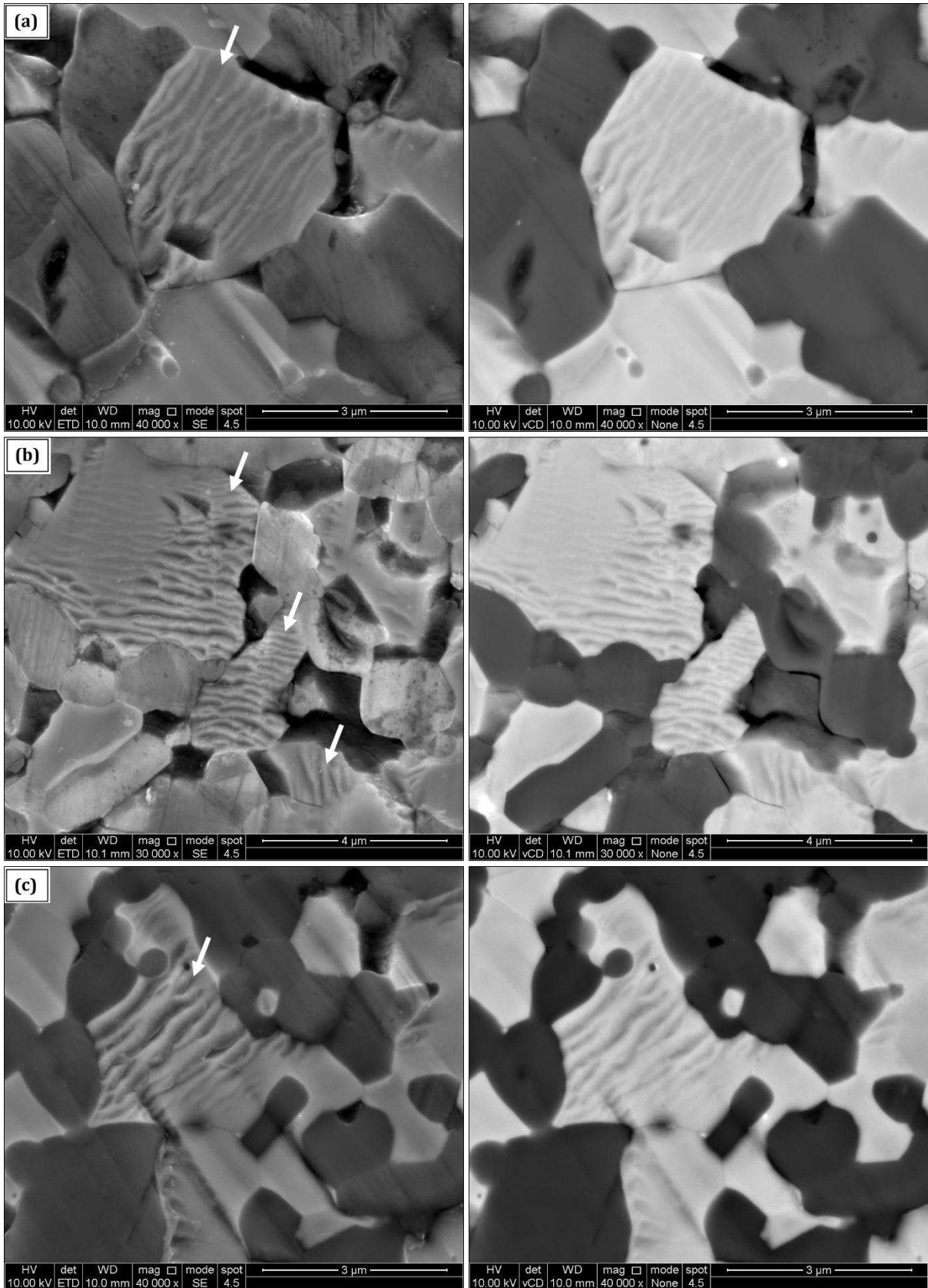


Fig. 5. Corresponding secondary electron (SE) and backscattered electron (BSE) micrographs of the worn surface morphology of the composite.

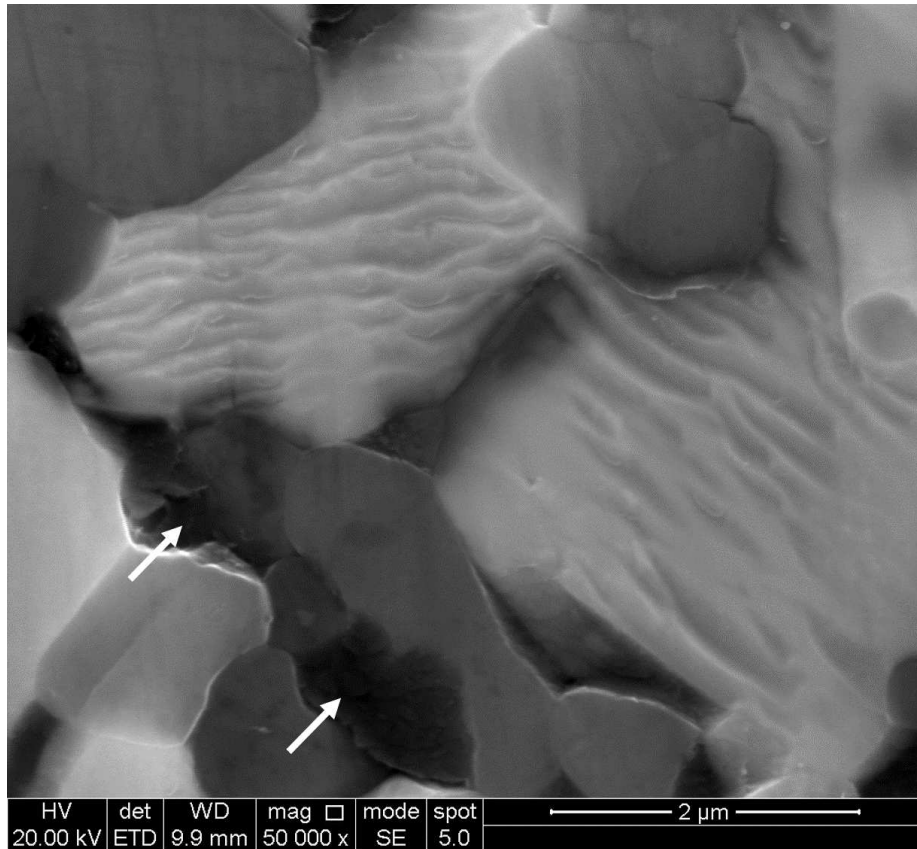


Fig. 6. Secondary electron (SE) micrograph showing the wear of the SiC grains (white arrow) leading to stress relaxation in the surrounding TiC grains evident as ripples.

To further characterize the ripple-like topographical feature observed on the TiC grain, SEM-image 3D reconstruction performed by converting an extracted area from the rippled TiC grain into a surface using MountainsSEM[®] is presented in Fig. 7. As shown, the ripple-like feature appears to be crystallographic, asymmetric and propagates along the sliding direction with varying amplitude as seen from the extracted curve of the line scan.

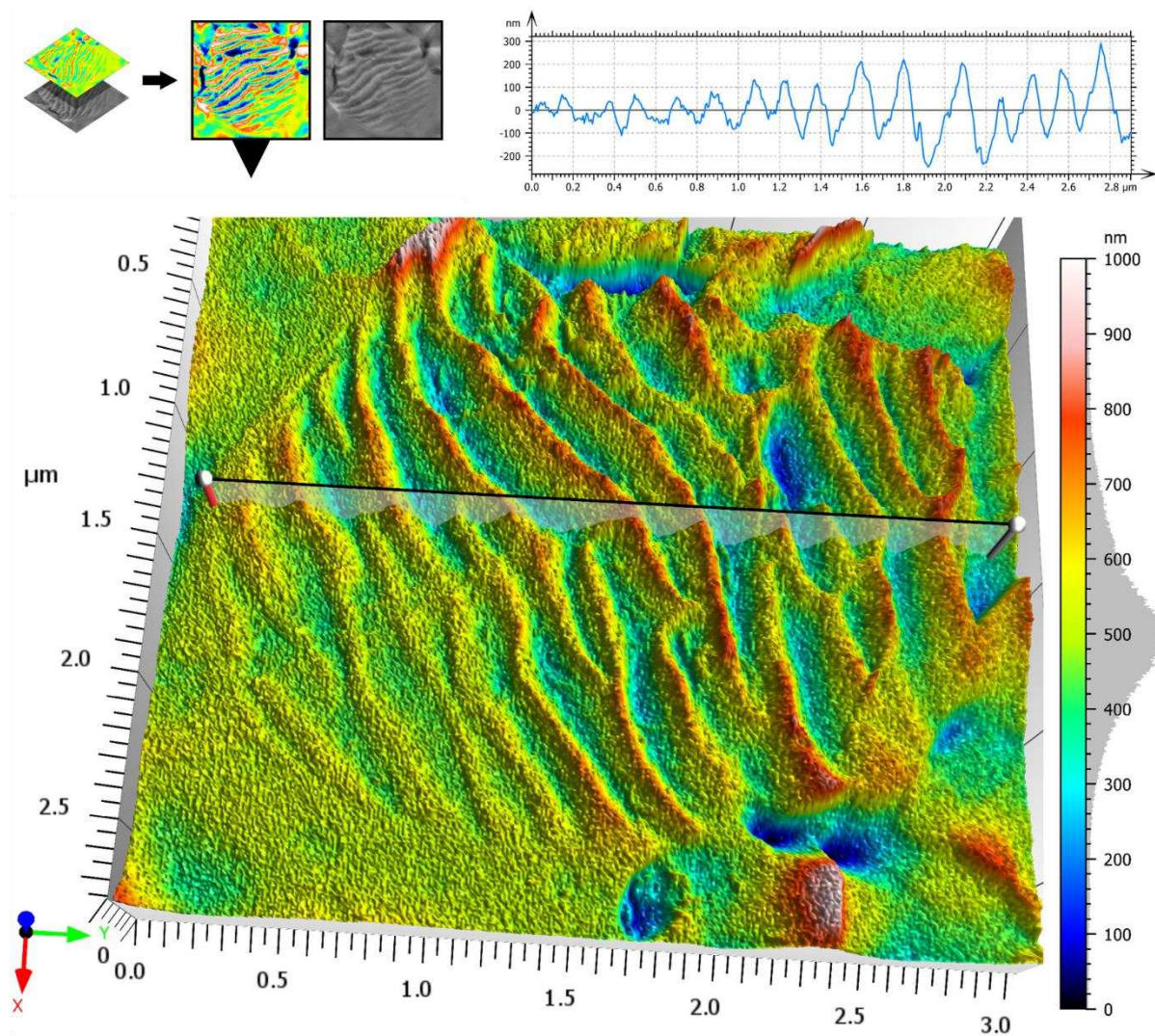


Fig. 7. SEM-3D reconstruction from a single image showing the 3D-view of the extracted surface and the profile line scan.

3.2.2. Transmission electron microscopy

Following site-specific in-situ FIB lift-out of a section from the localized rippled TiC grain, detailed analysis was undertaken using TEM to further investigate the ripple-like feature on the surface of the TiC grains. TEM analysis revealed what appears to be from all indications - especially judging from the diffraction pattern (Fig. 8(d)) and STEM/EDS analysis (Fig. 9) - an exfoliation of carbon from TiC; a mechanism that can be referred to as stress-relaxation induced mechanical exfoliation. Residual stress relaxation triggered by the superposition of an external stress [10] as well as mechanical exfoliation of graphite from carbon-based material [25] have already been reported elsewhere. It appears that stress relaxation led to bond relaxation in TiC which possesses a weaker Ti-C atom covalent bonding as compared to the very strong tetrahedral Si-C atom covalent bonding in SiC [26] making it easy for carbon

1
2
3
4
5
6
7
8
9
10
11
12
13
14
15
16
17
18
19
20
21
22
23
24
25
26
27
28
29
30
31
32
33
34
35
36
37
38
39
40
41
42
43
44
45
46
47
48
49
50
51
52
53
54
55
56
57
58
59
60
61
62
63
64
65

to be exfoliated preferentially from TiC during the sliding contact. The subsequent deformation of the exfoliated carbon following repeated sliding contact led to ripple formation as well as kink bands (Fig. 8(c)) – a deformation micromechanism. The diffraction pattern (Fig. 8(d)) obtained from the exfoliated carbon (white arrow in Fig. 8(a)) shows the characteristic graphite annular rings.

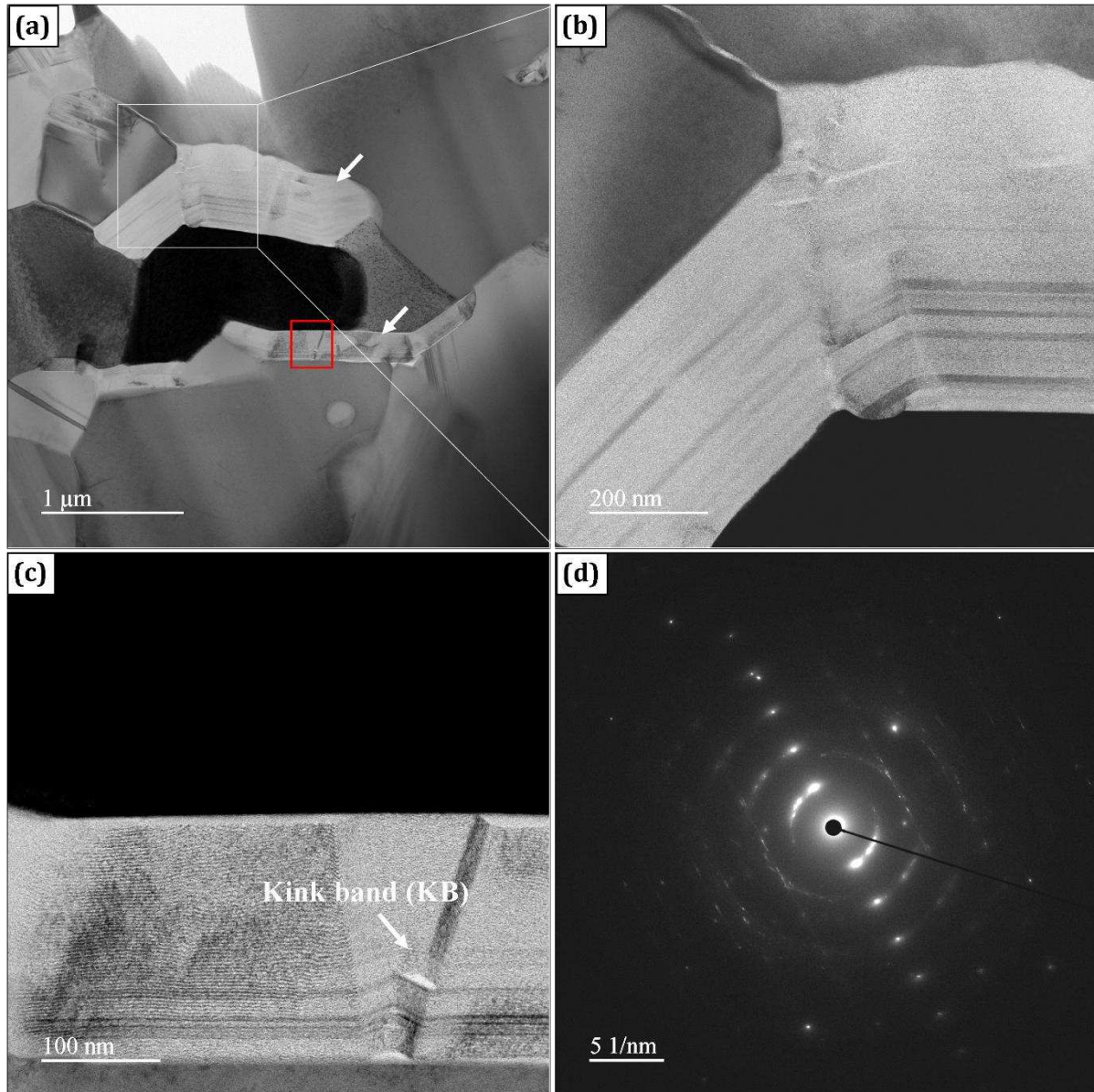
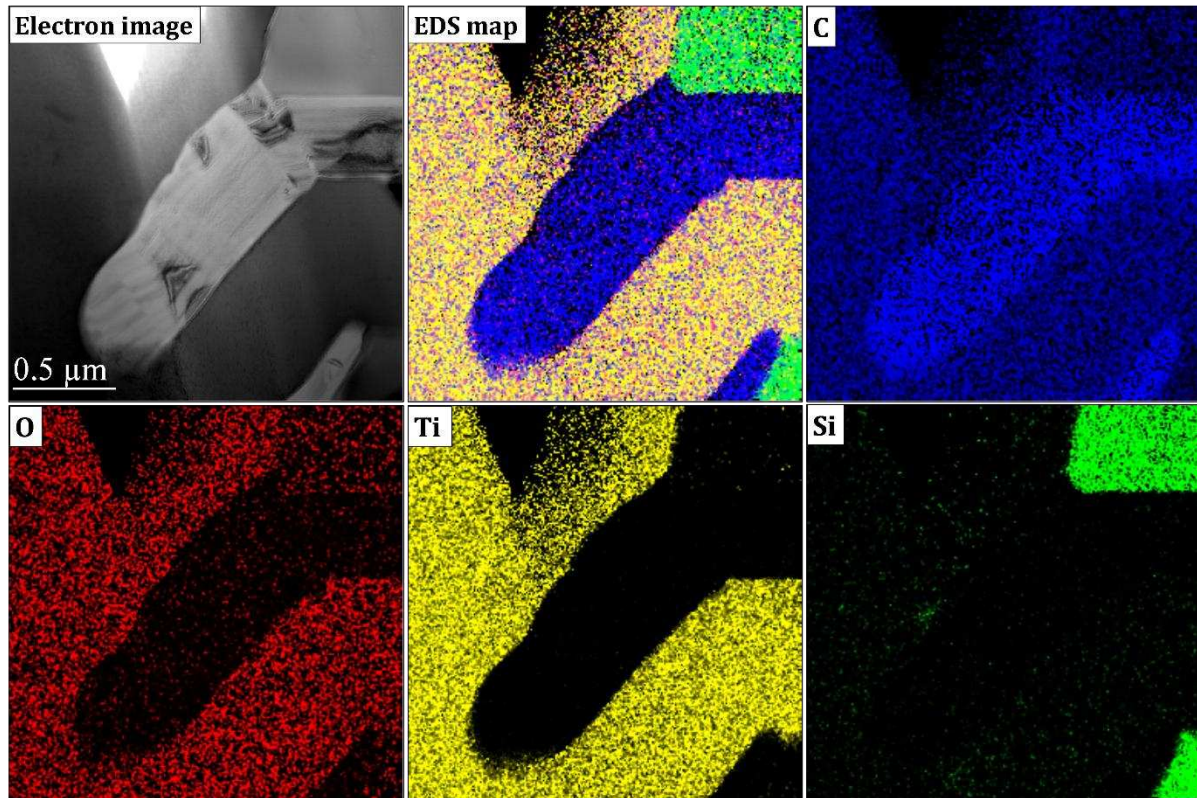


Fig. 8. TEM micrographs showing: (a) exfoliation of carbon from TiC; (b) higher magnification of highlighted section in (a); (c) higher magnification of highlighted red rectangle in (a) showing kink band (KB) formation, and (d) selected area electron diffraction (SAED) pattern showing graphite annular rings.

STEM/EDS elemental chemical mapping of the localized rippled region (Fig. 8(a)) is presented in Fig. 9. As shown, carbon-rich region following the mechanical exfoliation of

1 carbon from TiC is evident. This further corroborates the graphite annular rings as observed
2 from the electron diffraction pattern presented in Fig. 8(d). Further, the presence of oxygen in
3 the worn surface highlights the important role frictional heating-induced oxidation played in
4 the wear process owing to the dry-sliding test condition.
5
6



35
36 **Fig. 9.** STEM/EDS chemical mapping of the cross-sectional FIBed rippled region from the worn TiC
37 grain.
38

39
40 It is worth mentioning that the average coefficient of friction and wear rates for this
41 composite system were higher than that obtained for monolithic TiC albeit similar synthesis
42 parameters and tribological test conditions as reported elsewhere in our earlier work [22]. The
43 beneficial improvement in fracture toughness due to thermal expansion mismatch between
44 the matrix and particle phase as well as phase transformation toughening which should have
45 led to an improvement in friction and wear behaviour appeared to have been compromised
46 and/or rendered inactive by the incipient stress relaxation. Also, the absence of the ripple-like
47 feature in the worn surface morphology of the monolithic TiC following the wear test as
48 reported elsewhere in our previous work [22] showed that its evolution in the particulate TiC
49 phase in the composite system is linked essentially to the inherent residual stresses.
50
51
52
53
54
55
56
57

58 **4. Conclusions**

59
60
61
62
63
64
65

1 SiC–TiC ceramic matrix composite was synthesized by SPS powder metallurgy method
2 above the cubic – to – hexagonal SiC phase transformation temperature. The synthesized
3 sample contained high residual stresses originating from mismatch in thermal expansion
4 between the matrix and the particle phase as well as mismatch in thermal expansion
5 between the α and β SiC phases upon phase transformation. Hydrostatic tensile stresses generated
6 during the sliding contact which inadvertently is superimposed on the residual stresses
7 trapped in the composite led to tensile stress relaxation around the TiC grains upon the wear
8 of the compressive stress element surrounding the SiC grains. The evidence presented in this
9 work suggests the grain-scale microstructural phenomena involving the evolution of ripples is
10 linked to the mechanical exfoliation of carbon following the Ti–C atoms bond degradation
11 and its subsequent deformation.
12
13
14
15
16
17
18
19
20

21 **Acknowledgements**

22
23 Authors will like to acknowledge University of Sheffield Knowledge Exchange Scholarship
24 19/20 funded by the EPSRC Impact Acceleration Account. Authors also acknowledge
25 support from Mr Bin Zhang, Head of Product Management at Anton Paar Tritec Switzerland.
26 We further acknowledge the NHS UK and all health workers around the world for keeping us
27 safe during Covid-19 making it possible to carry out this study.
28
29
30
31
32

33 **References**

- 34
35 1. Ceramic Matrix Composite Toughening Mechanisms: An Update, in Proceedings of the 9th
36 Annual Conference on Composites and Advanced Ceramic Materials: Ceramic Engineering
37 and Science Proceedings. p. 589-607.
- 38 2. Lee, W.E. and M. Rainforth, Ceramic Microstructures: Property control by processing. 1994:
39 Springer Netherlands.
- 40 3. Mechanisms of Toughening in Ceramic Matrix Composites, in Proceedings of the 5th Annual
41 Conference on Composites and Advanced Ceramic Materials: Ceramic Engineering and
42 Science Proceedings. p. 661-701.
- 43 4. Filipuzzi, L., et al., Oxidation Mechanisms and Kinetics of 1D-SiC/C/SiC Composite
44 Materials: I, An Experimental Approach. Journal of the American Ceramic Society, 1994.
45 **77**(2): p. 459-466.
- 46 5. C/C-SiC Composites for Hot Structures and Advanced Friction Systems, in 27th Annual
47 Cocoa Beach Conference on Advanced Ceramics and Composites: B: Ceramic Engineering
48 and Science Proceedings. p. 583-592.
- 49 6. Yang, Z., et al., Microstructure and thermal physical properties of SiC matrix
50 microencapsulated composites at temperature up to 1900 °C. Ceramics International, 2020.
51 **46**(4): p. 5159-5167.
- 52 7. Rebillat, F., 20 - Advances in self-healing ceramic matrix composites, in Advances in
53 Ceramic Matrix Composites (Second Edition), I.M. Low, Editor. 2014, Woodhead
54 Publishing. p. 475-514.
- 55 8. Rice, R.W., R.C. Pohanka, and W.J. McDonough, Effect of Stresses from Thermal Expansion
56 Anisotropy, Phase Transformations, and Second Phases on the Strength of Ceramics. Journal
57 of the American Ceramic Society, 1980. **63**(11- 12): p. 703-710.
58
59
60
61
62
63
64
65

9. Davidge, R.W., Chapter 13 - The Mechanical Properties and Fracture Behaviour of Ceramic-Matrix Composites (CMC) Reinforced With Continuous Fibres, in Composite Materials Series, K. Friedrich, Editor. 1989, Elsevier. p. 547-569.
10. Amjad, K., et al., The interaction of fatigue cracks with a residual stress field using thermoelastic stress analysis and synchrotron X-ray diffraction experiments. Royal Society open science, 2017. **4**(11): p. 171100-171100.
11. Wei, G.C. and P.F. Becher, Improvements in Mechanical Properties in SiC by the Addition of TiC Particles. Journal of the American Ceramic Society, 1984. **67**(8): p. 571-574.
12. Prev y, P. and J. Cammett, The influence of surface enhancement by low plasticity burnishing on the corrosion fatigue performance of AA7075-T6. International Journal of Fatigue, 2004. **26**: p. 975-982.
13. Daou, E.E., The zirconia ceramic: strengths and weaknesses. The open dentistry journal, 2014. **8**: p. 33-42.
14. Fattahi, M., et al., Influence of TiB₂ content on the properties of TiC-SiCw composites. Ceramics International, 2019.
15. Chae, K.W., K. Niihara, and D.-Y. Kim, Improvements in the mechanical properties of TiC by the dispersion of fine SiC particles. Journal of Materials Science Letters, 1995. **14**(19): p. 1332-1334.
16. de Mestral, F. and F. Thevenot, Ceramic composites: TiB₂-TiC-SiC. Journal of Materials Science, 1991. **26**(20): p. 5547-5560.
17. Evans, A.G. and K.T. Faber, Toughening of Ceramics by Circumferential Microcracking. Journal of the American Ceramic Society, 1981. **64**(7): p. 394-398.
18. Chen, J., W. Li, and W. Jiang, Characterization of sintered TiC-SiC composites. Ceramics International, 2009. **35**(8): p. 3125-3129.
19. MoberlyChan, W.J., et al., The Cubic — To — Hexagonal Transformation to Toughen Sic, in Ceramic Microstructures: Control at the Atomic Level, A.P. Tomsia and A.M. Glaeser, Editors. 1998, Springer US: Boston, MA. p. 177-190.
20. Lin, B.-W., T. Yano, and T. Iseki, High-Temperature Toughening Mechanism in SiC/TiC Composites. Journal of the Ceramic Society of Japan, 1992. **100**(1160): p. 509-513.
21. Qian, X.K., 1 - Methods of MAX-phase synthesis and densification – I A2 - Low, I.M, in Advances in Science and Technology of Mn+1axn Phases. 2012, Woodhead Publishing. p. 1-19.
22. Magnus, C., T. Kwamman, and W.M. Rainforth, Dry sliding friction and wear behaviour of TiC-based ceramics and consequent effect of the evolution of grain buckling on wear mechanism. Wear, 2019. **422-423**: p. 54-67.
23. Pierson, H.O., Handbook of refractory carbides and nitrides : properties, characteristics, processing, and applications. 1996, Westwood, N.J.: Westwood, N.J. : Noyes Publications, c1996.
24. Heuer, A.H., et al., $\beta \rightarrow \alpha$ Transformation in Polycrystalline SiC: I, Microstructural Aspects. Journal of the American Ceramic Society, 1978. **61**(9- 10): p. 406-412.
25. Alaferdov, A., et al., Ripplcation in graphite nanoplatelets during sonication assisted liquid phase exfoliation. Carbon, 2017. **129**.
26. Smith, T.P. and R.F. Davis, Silicon Carbide, in Encyclopedia of Materials: Science and Technology, K.H.J. Buschow, et al., Editors. 2001, Elsevier: Oxford. p. 1-6.



DECLARATION OF INTEREST STATEMENT

We have no conflict of interest to disclose.